Published in final edited form as:

Biochemistry. 2023 February 07; 62(3): 710–721. doi:10.1021/acs.biochem.2c00658.

Discovery and mechanistic analysis of structurally diverse inhibitors of acetyltransferase Eis among FDA-approved drugs

Allan H. Pang[†],

Keith D. Green[†],

Ankita Punetha,

Nishad Thamban Chandrika,

Kaitlind C. Howard,

Sylvie Garneau-Tsodikova[*], **Oleg V. Tsodikov**[*]

Department of Pharmaceutical Sciences, College of Pharmacy, University of Kentucky, 789 South Limestone Street, Lexington, KY, 40536-0596, USA.

Abstract

Over one and a half million people die of tuberculosis (TB) each year. Multidrug-resistant TB infections are especially dangerous, and new drugs are needed to combat them. The high cost and complexity of drug development make repositioning of drugs that are already in clinical use for other indications a potentially time- and money-saving avenue. In this study, we identified among existing drugs five compounds: azelastine, venlafaxine, chloroquine, mefloquine, and proguanil as inhibitors of acetyltransferase Eis from *Mycobacterium tuberculosis*, a causative agent of TB. Eis upregulation is a cause of clinically relevant resistance of TB to kanamycin, which is inactivated by Eis-catalyzed acetylation. Crystal structures of these drugs as well as chlorhexidine in complexes with Eis showed that these inhibitors were bound in the aminoglycoside binding cavity, consistent with their established modes of inhibition with respect to kanamycin. Among three additionally synthesized compounds, a proguanil analogue, designed based on the crystal structure of the Eis-proguanil complex, was 3-fold more potent than proguanil. The crystal structures of these compounds in complexes with Eis explained their inhibitory potencies. These

[*]Correspondence to: sylviegtsodikova@uky.edu or oleg.tsodikov@uky.edu.
[†]These authors contributed equally to this work.

Author contributions

A.H.P., A.P., and O.V.T. performed the crystallographic studies. K.D.G. performed the microbiological and biochemical experiments. K.C.H. did the chemical synthesis of compounds **1**-**3**. N.T.C. verified the purity of compounds **1**-**3** and prepared corresponding figures. O.V.T. and S.G.-T. were responsible for the overall design, supervision, completion of the work, and writing of the manuscript. All authors contributed to the writing of their respective experimental section(s). All authors have read and approved of the manuscript and supporting information.

Declaration of competing interest

The authors declare that they have no known competing financial interests or personal relationships that could have appeared to influence the work reported in this manuscript.

SUPPORTING INFORMATION

^{1}H NMR, ^{13}C NMR, and MS spectra (Figures S1–S8), structures of compounds used in this study (Figure S9), dose response curves (Figure S10), omit map views of Eis-inhibitor interfaces (Figure S11), and superimposition of inhibitors with tobramycin (Figure S12). Tables for mode of inhibition (Table S1) and crystallographic statistics (Tables S2 and S3). The Supporting Information is available free of charge on the journal website.

These PDB IDs can also be found in Tables S2 and S3 in the Supporting Information.

UniProt ID: P9WFK7

initial efforts in rational drug repositioning can serve a starting point in further development of Eis inhibitors.

Graphical Abstract

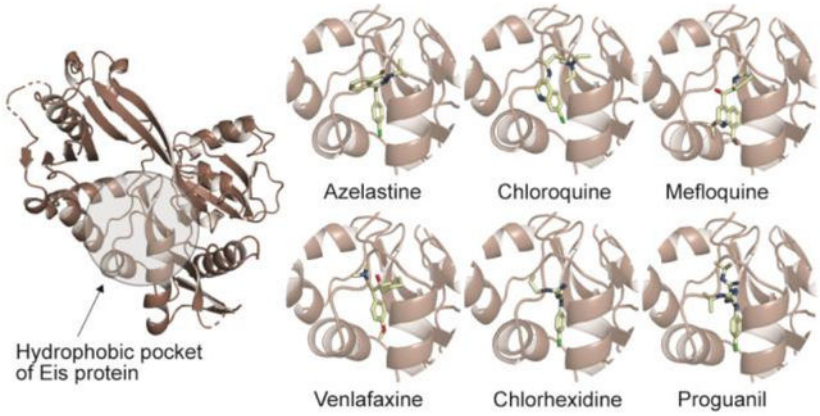

Keywords

crystal structure; drug repositioning; enzyme; medicinal chemistry; mode of inhibition

PDB IDs:

8F4U (Eis-AZL complex); 8F4W (Eis-VEN complex); 8F4Z (Eis-CHQ complex); 8F51 (Eis-MEF complex); 8F7A (Eis-CHX complex); 8F4T (Eis-PRO complex); 8F55 (Eis-1 complex); 8F57 (Eis-2 complex); 8F58 (Eis-3 complex)

INTRODUCTION

In 2021, an estimated 1.6 million people worldwide died of tuberculosis (TB).[1] TB is the second leading cause of death from an infectious disease, recently outpaced by the global COVID-19 pandemic.[1–3] In fact, COVID-19 reversed a recent trend of declining TB deaths, making it difficult to meet the goal of the World Health Organization (WHO) to end the global TB epidemic by 2035.[4] One of the biggest hurdles in combating TB is antibiotic resistance. Treatment of this disease requires the use of multiple antibiotics for an extended period of time: months or even years. As the *Mycobacterium tuberculosis* (*Mtb*) bacterium, the causative agent of TB, has evolved as an infection in the human host, drug-resistant strains have emerged due to problems with accurate diagnosis, availability of the drugs, and adherence to the treatment regimen. According to current Centers for Disease Control and Prevention (CDC) definitions, TB infections that are resistant to potent first-line drugs rifampicin and isoniazid (INH) are referred to as multidrug-resistant (MDR) TB, whereas MDR TB infections that are additionally resistant to a second-line injectable, such as aminoglycoside kanamycin (KAN) or amikacin, or a fluoroquinolone, are classified as pre-extensively drug-resistant (pre-XDR) TB. New efficacious anti-TB drugs are clearly needed to treat patients who have drug-resistant TB. To this end, our laboratory focused on developing small molecules that can inactivate *Mtb* enhanced intracellular survival (Eis)

enzyme. Eis protein (Rv2416c of *Mtb* strain H37Rv) is an acetyltransferase, which functions as a drug-resistance factor when upregulated, by transferring the acetyl group from acetyl coenzyme A (AcCoA) to an amino group of aminoglycosides such as second-line anti-TB drugs KAN and amikacin, inactivating them.[5–10] Eis is upregulated in clinically relevant aminoglycoside-resistant *Mtb* strains due to a mutation either in the *eis* promoter or in the 5'-untranslated region of the *whiB7* gene.[11–13] We successfully employed a biochemical assay in a high-throughput setting to discover several families of Eis inhibitors with diverse structural scaffolds:[14] isothiazole *S*,*S*-dioxides,[15] sulfonamides,[16] methyl 4*H*-furo[3,2-b]pyrrole-5-carboxylates and 3-(1,3-dioxolano)-2-indolinones,[17] pyrrolo[1,5-a]pyrazines,[18] 1,2,4-triazino[5,6b]indole-3-thioethers,[19] thieno[2,3-d]pyrimidines,[20] substituted benzyloxy-benzylamines,[21] and haloperidol (HAL) derivatives.[22] Our numerous crystal structures of Eis in complex with these inhibitors[15, 16, 18, 20, 22] revealed a "druggable" hydrophobic pocket in the substrate binding site occupied by inhibitor moieties, providing a mechanistic rationale for the mode of action of the inhibitors and helping design them. The Eis inhibitors discovered thus far obstructed proper binding of the aminoglycoside substrate, as concluded based on the superimposition of the structures of Eis-inhibitor and Eis-tobramycin (TOB) complexes.[7] Representatives of different structural families of the Eis inhibitors decreased or abolished KAN resistance of the clinically relevant KAN-resistant *Mtb* strain (K204) in culture. Our preliminary safety studies showed that some of these inhibitors lacked mammalian cytotoxicity. The potency and lack of toxicity make these molecules promising leads for development as aminoglycoside adjuvants in MDR TB treatment. To accelerate the drug development process, repositioning existing FDA-approved drugs beyond their intended original use has been one of the approaches in the pharmaceutical industry. For example, the repositioning strategy allows a highly informed approach to safety testing for a new use, since safety and pharmacokinetic information for the approved use is already available.[23, 24] We recently found that HAL, an FDA-approved antipsychotic drug, was an Eis inhibitor and generated a series of HAL analogues in search of anti-TB compounds and KAN adjuvants.[22] In this study, we identified five other FDA-approved drugs as Eis inhibitors: the antihistamine azelastine (AZL), the antidepressant venlafaxine (VEN), and the antimalarial drugs chloroquine (CHQ), mefloquine (MEF), and proguanil (PRO).

MATERIALS AND METHODS

Materials and instrumentations.

Azelastine (AZL), venlafaxine (VEN), chloroquine (CHQ), mefloquine (MEF), proguanil (PRO), and the additional 20 FDA-approved compounds used for screening were purchased from Millipore-Sigma (St. Louis, MO, USA) or AK Scientific (Union City, CA, USA). Acetylation activity assays were performed using a multimode SpectraMax M5 plate reader from Molecular Devices (Sunnyvale, CA, USA) and 96-well plates from Greiner (Monroe, NC, USA). Reagents for Eis inhibition assays such as Ellman's reagent, Tween® 80, KAN, neomycin B (NEO), acetyl-CoA (AcCoA), and chlorhexidine (CHX) were purchased from Sigma-Aldrich (St. Louis, MO, USA). Resazurin was also purchased from Sigma-Aldrich (Milwaukee, WI, USA). *Mtb* $mc^2$6230 was a gift from Prof. William Jacobs Jr. (Albert Einstein College of Medicine, NY, USA), and the *Mtb* $mc^2$6230 K204 strain was generated in our laboratory.[22] The chemicals used for synthesis were purchased from Sigma-Aldrich

(St. Louis, MO), TCI America (Portland, OR), and Chem-Impex (Wood Dale, IL), and used without any further purification. Chemical reactions were monitored by TLC (Merck, silica gel 60 F_{254}) and visualization was achieved using UV light. Compounds were purified by SiO_2 flash chromatography (Dynamic Adsorbents Inc., flash SiO_2 gel 32–63μ). ^1H and ^{13}C NMR spectra were recorded on an Agilent MR-400 spectrometer using deuterated solvents as specified. Chemical shifts (δ) are given in parts per million (ppm). Coupling constants (*J*) are given in Hertz (Hz), and conventional abbreviations used for signal shape are as follows: s; singlet; d, doublet; dd, doublet of doublets; dt, doublet of triplets; m, multiplet; td, triplet of doublets. High resolution-mass spectrometry (HRMS) was carried out using a Shimadzu prominence LC system equipped with an AB SCIEX Triple TOFTM 5600 mass spectrometer (Shimadzu manufacturing, Kyoto, Japan). HRMS $[M+H]^+$ signals were consistent with the expected molecular weights for the reported compounds.

Synthesis and characterization of compound 1 (SGT1614).

A solution of 4-chlorobenzaldehyde (100 mg, 0.71 mmol), aminoguanidine hydrochloride (94 mg, 0.85 mmol), and a catalytic amount of HCl (0.04 mL) was stirred in anhydrous EtOH (5 mL). The resulting mixture was refluxed at 90 °C for 2 h. The organic solvents were removed *in vacuo* after the reaction was complete as determined by TLC (hexanes:EtOAc/3:1, R_f 0.26). The residue obtained was suspended in CH_2Cl_2 (10 mL), filtered, and concentrated to yield the pure compound **1** (0.21 g, quant.) as a white solid: ^1H NMR (400 MHz, CD_3OD, Figure S1) δ 8.08 (s, 1H, aromatic), 7.80 (d, J = 8.6 Hz, 2H, aromatic), 7.46 (d, J = 8.6 Hz, 2H, aromatic); ^{13}C NMR (100 MHz, CD_3OD, Figure S2) δ 157.3, 148.2, 137.9, 133.6, 130.3 (2C), 130.2 (2C); HRMS *m/z* calcd for $C_8H_9ClN_4$ $[M+H]^+$: 197.0594; found 197.0596 (Figure S3).

Synthesis and characterization of compound 2 (SGT1615).

A solution of 4-chlorobenzaldehyde (100 mg, 0.71 mmol), 3-fluorophenylhydrazine hydrochloride (139 mg, 0.85 mmol), and a catalytic amount of HCl (0.04 mL) was stirred in anhydrous EtOH (5 mL). The resulting mixture was refluxed at 90 °C for 2 h. The organic solvents were removed *in vacuo* after the reaction was complete as determined by TLC (hexanes:EtOAc/3:1, R_f 0.25). The residue obtained was suspended in CH_2Cl_2 (10 mL), filtered, and concentrated. The crude product was purified by column chromatography (SiO_2 gel, hexanes:EtOAc/3:1) to yield compound **2** (79 mg, 45%) as a pink solid: ^1H NMR (400 MHz, CD_3OD, Figure S4) δ 7.76 (s, 1H, aromatic), 7.63 (d, J = 8.6 Hz, 2H, aromatic), 7.36 (d, J = 8.6 Hz, 2H, aromatic), 7.17 (td, J_1 = 8.2 Hz, J_2 = 6.6 Hz, 1H, aromatic), 6.86 (dt, J_1 = 11.6 Hz, J_2 = 2.3 Hz, 1H, aromatic), 6.80 (dd, J_1 = 8.2 Hz, J_2 = 2.1 Hz, 1H, aromatic), 6.46 (td, J_1 = 8.7 Hz, J_2 = 2.6 Hz, 1H, aromatic); ^{13}C NMR (100 MHz, $CDCl_3$, Figure S5) δ 165.4, 163.0, 146.4, 146.3, 136.9, 134.6, 133.7, 130.7 (J = 9.9 Hz, 1C), 129.1, 127.6, 108.5 (J = 2.6 Hz, 1C), 107.0 (J = 21.6 Hz, 1C), 100.3 (J = 26.5 Hz, 1C); HRMS *m/z* calcd for $C_{13}H_{10}ClFN_2$ $[M+H]^+$: 249.0595; found 249.0598 (Figure S6).

Synthesis and characterization of compound 3 (SGT1616).

A solution of 4-chlorobenzaldehyde (100 mg, 0.71 mmol), 4-fluorophenylhydrazine hydrochloride (138 mg, 0.85 mmol), and a catalytic amount of HCl (0.04 mL) was stirred in

anhydrous EtOH (5 mL). The resulting mixture was refluxed at 90 °C for 2 h. The organic solvents were removed *in vacuo* after the reaction was complete as determined by TLC (hexanes:EtOAc/1:1, R_f 0.81). The residue obtained was suspended in CH_2Cl_2 (10 mL), filtered, and concentrated. The crude product was purified by column chromatography (SiO_2 gel, hexanes:EtOAc/1:1) to yield compound **3** (146 mg, 82%) as a red solid: ^{1}H NMR (400 MHz, CD_3OD, Figure S7) δ 7.73 (s, 1H, aromatic), 7.61 (d, J = 8.6 Hz, 2H, aromatic), 7.34 (d, J = 8.5 Hz, 2H, aromatic), 7.08–7.04 (m, 2H, aromatic), 6.98–6.93 (m, 2H, aromatic); ^{13}C NMR (100 MHz, $CDCl_3$, Figure S8) δ 191.1, 141.0, 136.2, 134.3, 134.0, 131.1, 129.7, 129.5, 129.1, 127.7, 127.4, 116.1 (J = 22.6 Hz, 1C), 114.0 (J = 7.4 Hz, 1C).

The acetylation activity assay to measure Eis inhibition.

The established acetylation assay using Ellman's reagent[14] was utilized to identify inhibitors of *Mtb* Eis in (1) a high-throughput manner, as previously described, using a ~2,500 compound library,[14] and (2) in 96-well plates using 20 FDA-approved selected drugs. The 20 FDA-approved drugs were selected based on structural details of Eis inhibitors we previously published.[25] In this assay, the reaction mixture contained Tris-HCl pH 8.0 (50 mM), Eis (0.25 μM), NEO (100 μM), AcCoA (40 μM), DTNB (0.5 mM), and a compound from the library (20 μM). These reaction assays were carried out in a clear 96-well plate and monitored at 412 nm. Confirmation was carried out in triplicate by retesting the inhibitors in a concentration-dependent manner. Five compounds: AZL, VEN, CHQ, MEF, and PRO were identified as confirmed hits. For these five hits, the IC_{50} values were determined in a reaction assay using the aminoglycoside KAN as an Eis substrate. Briefly, Eis (0.25 μM), KAN (100 μM), and the hit compound were first mixed in Tris-HCl pH 8.0 (50 mM) and incubated for 10 min at room temperature. AcCoA (0.5 mM) and Ellman's reagent (2 mM) were added to the reaction mixture to initiate the acetylation process. The concentration noted in parentheses are all final concentrations. All assays were carried out in triplicate. The mean values of the data were normalized to the value of the activity in the absence of an inhibitor (not included in the plots). The data were analyzed by nonlinear regression using a dose-response curve in SigmaPlot 14.0. A four-parameter logistic curve was used to fit the data, where the maximum and the minimum of the activity, IC_{50} and the Hill coefficient were fitting parameters. The chemical structures of the 20 FDA-approved compounds tested and the two compound hits from the ~2,500 compound library are shown in Figure S9. The IC_{50} values for AZL, VEN, CHQ, MEF, and PRO are listed in Table 1. The corresponding IC_{50} curves are presented in Figure S10.

Crystallization of the Eis-inhibitor complexes.

The *Mtb* Eis C204A protein was produced and purified according to our previously reported protocol.[22] Crystallization of *Mtb* Eis C204A was carried out following the procedure described before.[5] Briefly, Eis crystals grown in the presence of KAN (10 mM) and CoA (8 mM) were obtained after two weeks by the hanging drop method (in drops containing a 1:1 ratio of protein solution:reservoir solution) and then equilibrated against the reservoir solution (Tris-HCl pH 8.5 (0.1 M), PEG 8,000 (10% *w*/*v*), and $(NH_4)_2SO_4$ (0.5 M)) at 21 °C. After that, KAN, CoA, and $(NH_4)_2SO_4$ were gradually removed by transferring crystals in a stabilization solution of Tris-HCl pH 8.5 (0.1 M) and PEG 8,000 (10% *w*/*v*). Crystals were allowed to stabilize for at least 10 min before they were gradually transferred to a

cryoprotectant solution with the same composition as the stabilization solution, additionally containing an inhibitor (1 mM) and 20% glycerol. The crystals were incubated in this solution in the presence of AZL, VEN, CHQ, MEF, CHX, and PRO, and its analogues **1**-**3** for at least 30 min before being rapidly frozen by plunging in liquid nitrogen.

Data collection and structure determination.

X-ray diffraction images were recorded on the Eiger 16M detector at the 22-ID beamline of the Advanced Photon Source at Argonne National Laboratory (Argonne, IL) at 100 K. The collected datasets were processed using HKL2000 suite.[26] Initial models were produced for all collected data by molecular replacement using Phaser[27] in the CCP4 suite. The crystal structure of CoA-*Mtb* Eis complex (PDB: 3R1K)[5] was used as the search model. All initial structures were assessed for the presence of unmodelled electron density in F_o-F_c electron density maps contoured above 2.0σ, to identify bound inhibitors. The structures were improved by several rounds of manual adjustment using WinCoot[28] and crystallographic refinement *via* Refmac.[29] Water molecules as well as different ligands present in the crystallization condition such as PEG, DMSO, and glycerol were then built into the structure. The stereochemistry of the refined structures was verified using MolProbity.[30] The data collection and structure refinement statistics are presented in Tables S2 and S3. The atomic coordinates and structure factor amplitudes of the refined Eis-inhibitor complex structures were deposited in the RCSB PDB website with IDs given in Tables S2 and S3.

Inhibition mode analysis.

The steady-state rates of acetylation (V) were measured as described for IC_{50} measurements, as a function of concentration of KAN for several concentrations ([I]) of AZL, CHQ, MEF, PRO, and compounds **1** and **2**, as specified. For each inhibitor, all the data were first analyzed simultaneously by a global nonlinear regression fit using SigmaPlot 14.0 using the mixed inhibition mode with the equilibrium constants for inhibitor binding free enzyme (K_i) and for inhibitor binding the enzyme-substrate complex ($K_{i,u}$) as fitting parameters. The Michaelis-Menten parameter values for the enzyme in the absence of the inhibitor ($K_{m,0}$ and $V_{max,0}$) were also fitting parameters. The following mixed inhibition rate law was used in this analysis:

$$V = \frac{V_{m,app}[KAN]}{K_{m,app} + [KAN]}, \quad (1)$$

where

$$V_{m,app} = V_{m,0}\frac{1}{1 + \frac{[I]}{K_{i,u}}} \quad (2)$$

$$K_{m,app} = K_{m,0}\frac{1 + \frac{[I]}{K_i}}{1 + \frac{[I]}{K_{i,u}}} \quad (3)$$

Where this mixed mode analysis was established not to be statistically justified (only the K_i or the $K_{i,u}$ value could be determined), we analyzed the data using the competitive or the uncompetitive mode, respectively. The best-fit values of K_i or $K_{i,u}$ are given in Table 1.

MIC determination.

The anti-*Mtb* activity of the 5 hits (AZL, VEN, CHQ, MEF, and PRO) and the three synthesized compounds (**1**, **2**, and **3**) was determined by testing the effect of the compounds on the growth of *Mtb* $mc^2$6230 and its K204 variant. The *Mtb* strains were grown in 7H9 broth supplemented with tyloxapol (0.05%), glycerol (0.5%), OADC (10%), casamino acids (0.2%), and pantothenate (24 μg/mL). The mycobacterial strains were grown on agar plates corresponding to the broth. Cells were transferred from the plates to the corresponding liquid medium until the attenuance at 600 nm was equal to that of a 0.5 McFarland standard. The culture was then diluted 1:100 and added to the compounds dissolved in the appropriate medium. Plates were incubated at 37 °C until growth was observed in the wells containing no compound (1–2 weeks). To assess the growth inhibition, 5 μL of a 2.5 mg/mL solution of resazurin was added to each well. Color change for each well was observed after an overnight incubation at 37 °C. We also determined the MIC value of KAN in the presence of the compounds listed above to identify if the hit compounds could be used as KAN adjuvant against *Mtb* $mc^2$6230 and K204 strains. Here, we followed the same procedure as above, except for the addition of KAN in the medium. For instance, the 1:100 dilution (100 μL) of the bacterial culture was added to the KAN (10–1.25 μg/mL) per compound (½× MIC concentration) mixture. These MIC data were measured in duplicate and are listed in Table 1.

Inhibitor selectivity.

AZL, CHQ, MEF, PRO, and compounds **1**, **2**, and **3** were also tested at a concentration of 200 μM with a variety of acetylating enzymes to identify if these molecules were selective inhibitors of *Mtb* Eis. They were tested against three aminoglycoside acetyltransferases (AACs): AAC(2')-Ic, AAC(3)-IV, and AAC(6')-Ie/APH(2")-Ia. Production and purification of these enzymes were reported previously.[5, 31] The conditions of the acetylation assays used for determination of IC_{50} values were the optimum conditions for each enzyme. Compounds were dissolved in buffer (MES pH 6.6 (50 mM) for AAC(6')-Ie/APH(2")-Ia and AAC(3)-IV, and sodium phosphate pH 7.4 (100 mM) for AAC(2')-Ic). Enzyme (0.25 μM for AAC(6')-Ie/APH(2")-Ia, and 0.125 μM for AAC(3)-IV and AAC(2')-Ic), NEO (100 μM), and AcCoA (150 μM) were used in these assays. The experiments with AAC(3)-IV and AAC(2')-Ic were performed at 25 °C. The assays with AAC(6')-Ie/APH(2")-Ia were run at 37 °C. All other methods and concentrations were the same as for the assays with Eis.

RESULTS AND DISCUSSION

Discovery of Eis inhibitors among FDA-approved drugs.

We recently reported a discovery of the antipsychotic FDA-approved drug HAL as an Eis inhibitor by testing a ~2,500-compound library using an established aminoglycoside acetyltransferase assay.[22] Among the compounds from the same library, we also identified AZL (Figure 1A) as a hit with a signal-to-noise ratio greater than 3. AZL is a phthalazine

derivative and a commonly used antihistamine, delivered either as intranasal spray for allergic and vasomotor rhinitis or eye drops for treatment of allergic conjunctivitis.[32] With HAL and AZL identified as HTS hits, we decided to test for Eis inhibition other FDA-approved compounds that had similar sizes and diverse chemical features (Figure S9). We included in this set antidepressants trimipramine (TRI), imipramine (IMP), maprotiline (MPT), and amitriptyline (AMI), an antipsychotic triflupromazine (TFZ), an antimalarial drug halofantrine (HFT), and a muscle relaxant cyclobenzaprine (CBP). We tested antidepressants mirtazapine (MRZ) and mianserin (MNS) to check if bulky tetracyclic compounds could inhibit Eis. We also included in this library a beta blocker propranolol (PPN) and antimalarial agents mefloquine (MEF) and chloroquine (CHQ). CHQ contains a halogenated aromatic ring system. A halogenated phenyl group was shown to be an important pharmacophore in other Eis inhibitor families,[15, 16, 18–22, 25] which prompted us to also include an antimalarial drug proguanil (PRO). Other compounds we tested were an anesthetic drug procaine (PRC) and a heart medicine procainamide (PCA), which contained an aniline group. In addition, we tested an antimalarial venlafaxine (VEN) and an anesthetic lidocaine (LDC), which bore methoxy and two methyl substituents on their phenyl rings, respectively. Finally, we chose to include beta blockers with a central phenyl ring betaxolol (BTX) and metoprolol (MPL). We tested the above compounds for inhibition of NEO acetylation activity of *Mtb* Eis at low-μM concentrations. We found that, in addition to AZL, four of the compounds, VEN, CHQ, MEF, and PRO (Figures 1A and S9) displayed detectable inhibition at the conditions of the original high-throughput assay. AZL, CHQ, and PRO contain a halogenated aromatic group. The discovery of MEF and VEN as Eis inhibitory hits revealed scaffolds that were not previously found among Eis inhibitors. To validate these five inhibitory hits, we carried out dose-response assays measuring acetylation of aminoglycoside KAN by Eis at different concentrations of the compounds prepared from fresh powders (Figure S10). In this set, AZL was the most potent inhibitor, with an IC_{50} value of 0.79 ± 0.08 μM, followed by MEF with an IC_{50} value of 4.2 ± 0.8 μM (Table 1). CHQ, PRO, and VEN were the weakest Eis inhibitors in this set, with IC_{50} values of 20 ± 2 μM, and 30 ± 7 μM, and 134 ± 21 μM respectively.

Crystal structures of Eis in complexes with AZL, CHQ, MEF, and VEN.

To study the mechanism of inhibition exerted by the five newly discovered Eis inhibitors as well as chlorhexidine (CHX), a topical antiseptic drug discovered as an Eis inhibitor previously[14] similar in structure to PRO (Figure S9), we determined crystal structures of the complexes of Eis with these six compounds (Tables S2 and S3). The crystals of these Eis-inhibitor complexes diffracted in the resolution range of 1.9 to 2.4 Å. The inhibitors were defined well by the strong omit F_o-F_c electron density maps (Figure S11), except for the azepanyl moiety of AZL and a part of the bound CHX. The absence of these moieties in the electron density was likely due to the lack of strong interactions of these moieties with Eis resulting in their rotational flexibility, leading to disorder of these regions in the crystals.

The inhibitors occupied sites that overlapped with or that were in the immediate vicinity of the aminoglycoside binding site of Eis (Figures 2A,B and S12),[7, 15] as was observed with other Eis inhibitors we previously reported. This inhibitor binding site included a hydrophobic pocket lined by side chains of several hydrophobic residues including Trp36

and Phe84 (Figure 2B–F). The Eis inhibitors reported so far were shown by kinetic studies to be competitive with the aminoglycoside substrate.[19–22] This mode of inhibition was explained by a spatial overlap of the bound inhibitors with the bound aminoglycoside substrate observed in the crystal structure of the Eis-TOB complex (Figures 2B and S12).[7] The hydrophobic pocket snugly accommodated the chlorophenyl ring of AZL (Figure 2C), the substituted quinoline moieties of CHQ (Figure 2D) and MEF (Figure 2E), and the methoxyphenyl ring of VEN (Figure 2F). These rings and ring systems of the inhibitors were nearly superimposable with each other and coplanar, interacting with nonpolar side chains of Leu63, Val40, Phe27, and Ala33, and sandwiched between Trp36 and Phe84. Standing out was the methoxy group of VEN, where the oxygen atom was in a dehydrated hydrophobic environment of the above residues, lacking a potential hydrogen bond donor. The loss of one or two potential hydrogen bonds upon binding Eis could explain the low inhibitory potency of VEN. The position of the chlorophenyl moiety of AZL in this hydrophobic pocket was similar to those of phenyl groups of our previously reported inhibitors (PDB IDs: 5EBV,[15] 6P3U,[25] 6X6Y,[22] 6X10,[22] 6X7A,[22] 6X6I,[22] and 6X6G[22]). For VEN, the phenyl ring was slightly rotated with respect to that of AZL, to fit the methoxy group in the binding pocket. The chloroquinoline moiety of CHQ was bound so that its chlorinated ring was superimposable with the methoxyphenyl ring of VEN. Although both MEF and CHQ contained a quinoline group, the 2,8-bis(trifluoromethyl)quinoline of MEF did not adopt a similar orientation to that of CHQ. Instead, it was wedged deeply in the hydrophobic pocket. The binding of this moiety caused a concerted movement of an Eis helix (residues 27–39), where the backbone atoms shifted by as much as 2.7 Å, to enlarge the pocket to accommodate the bulky substituted quinoline. As a result, one trifluoro group interacted with the side chains of Phe27, Phe17, and Ala33, while the other trifluoromethyl occupied the hydrophobic pocket lined by Phe84, Leu63, Val40, and Arg37. We suggest that this considerable remodeling of the substrate binding region by MEF contributes to its inhibitory potency, despite a relatively minor steric overlap with the bound TOB substrate from our prior structure.

The remaining chemical moieties of the inhibitors were bound in a shallow region of the binding site that was adjacent to or overlapping with the aminoglycoside binding site (Figure S12). The 2-methylphthalazinone of AZL was held by perpendicular stacking interactions with the indole ring of Trp36 on one side and the phenyl ring of Phe27 on the other (Figure 2C). The N-2 nitrogen atom of the 2-methylphthalazinone was located appropriately for hydrogen bonding with the hydroxyl group of Ser83 and the C-terminal (Phe402) carboxyl group. The oxygen atom, on the other hand, formed a hydrogen bond with a nearby water molecule, which in turn was bonded to the carboxyl group of Asp26. The azepanyl moiety was mostly disordered with only two of its carbon chains placed in the electron density map (Figure S11A). The azepanyl moiety protruded into a solvent filled entrance to the binding site, which was additionally occupied by several bound water molecules and a glycerol molecule from the cryoprotectant solution (Figure 2C); therefore, the disorder of this largely hydrophobic moiety was unsurprising. In the structure of the Eis-MEF complex (Figure 2E), the 2-piperidylethanol group of MEF occupied the site where the 2-methylphthalazinone of AZL was bound, with the piperidyl ring rotated by about 90° with respect to the 2-methylphthalazone. The nitrogen of the piperidyl ring of MEF formed a water mediated

hydrogen bond with the C-terminal carboxyl group of Eis. We previously showed that the C-terminal carboxyl group was essential for catalysis.[5] The engagement of AZL and MEF with the C-terminal carboxyl group observed in these structures explain the observed potent inhibition of Eis by these two drugs. The aliphatic part of the piperidyl ring of MEF was in the hydrophobic environment of the aromatic side chains of Phe84, Phe24, and Phe27. The piperidyl spatially overlaps the aminoglycoside binding site observed in our reported structure of the Eis-TOB complex (Figure S12C). The greater degree of this overlap for AZL than for MEF due to the bulky methylated azepanyl group may explain the higher potency of AZL compared to that of MEF. In the Eis-VEN complex (Figure 2F), the cyclohexane ring of the VEN was located and oriented similarly to the piperidyl ring of MEF. The hydroxyl group of VEN was positioned appropriately to form a hydrogen bond with the carboxyl group of Asp26, whereas the cyclohexane ring abutted the phenyl ring of Phe24. The respective part of CHQ located in the substrate binding site is highly flexible, which may account for the relatively weak inhibition of Eis by this molecule. In the Eis-CHQ structure (Figure 2D), the nitrogen atom of the *N,N*-diethyl group formed a salt bridge with the carboxyl group of Asp26, while the two ethyl groups interacted with the phenyl ring of Phe24.

Crystal structures of Eis in complexes with CHX and PRO.

We previously reported that CHX (Figure S9C) exhibited sub-μM inhibition of Eis (Table 1).[14] In fact, CHX had a similar potency to that of AZL, which also contained a chlorophenyl moiety. In this study, we were surprised to learn that PRO, a structural relative of CHX, was a 45-fold weaker Eis inhibitor than CHX. In the crystal structure of the Eis-CHX complex determined here (Table S3, Figure 3A), one chlorophenyl group, the adjacent biguanide group and a half of the linker were ordered, whereas the other half of the molecule was disordered (Figure S11E). The disordered part, regardless of its conformation must occupy the aminoglycoside binding site (Figure S12E). The chlorophenyl group was bound in the hydrophobic pocket similarly to that of AZL. The positively charged biguanide formed a strong salt bridge with the carboxyl group of Asp26. The side chain of Asp26 was in a different rotamer state than in the complex with AZL apparently to form this salt bridge. The three methylene groups of the linker made nonpolar contacts with the indole ring of Trp36. On the other hand, in the crystal structure of the Eis-PRO complex (Table S3, Figure 3B), the bound PRO was observed in two equally occupied conformations (Figures 3B and S11F). In both conformations, the chlorophenyl group was bound to Eis the same way, similarly to the respective group of CHX, and the guanidinyl adjacent to this group stacked onto the indole ring of Trp36. The second guanidinyl-isopropyl moiety was bound in two conformations. This was apparently a result of the presence of an isopropyl group in this molecule. One of the conformations was like that of CHX, where a biguanide-Asp26 salt bridge was present. However, in this conformation the methyl group of PRO (not present in CHX) was in the hydrophilic environment of the hydroxyl group of Ser32 and the backbone amide nitrogen of Ala33, which likely made this conformation unstable. In the other conformation, the biguanide formed a salt bridge with the C-terminal carboxyl group, while the isopropyl group was in a negatively charged environment of the carboxyl groups of Asp26 and Glu401, lacking a suitable hydrophobic pocket. These unfavorable interactions of the bound PRO likely explain why it is a much less potent inhibitor of Eis than CHX.

Design of PRO/CHX analogues and crystal structures of Eis-analogue complexes.

Due to reported toxic effects of CHX,[33] this molecule could not be used systemically. We then asked if a similar potency could be achieved by making relatively simple compounds containing a *p*-chlorophenyl group in combination with a guanidinyl or another halophenyl group. We designed three analogues where a guanidinyl, an *m*-fluorophenyl, and *p*-fluorophenyl (compounds **1**-**3**, respectively; Figure 1B) were connected to a *p*-chlorophenyl group *via* a hydrazone linkage. Compound **1** was designed based on the crystal structure of the Eis-PRO complex with an idea of removing the isopropyl group while preserving a positively charged guanidinyl. These three compounds were generated using a linear one-step synthesis (Figure 1B). The commercially available 4-chlorobenzaldehyde was stirred in ethanol and concentrated hydrochloric acid with aminoguanidine hydrochloride, 3-fluorophenylhydrazine hydrochloride, and 4-fluorophenylhydrazine hydrochloride to form hydrazone derivatives **1**-**3** in 45%-quantitative yields, respectively. These three compounds were dissolved in DMSO and tested for the inhibition of Eis analogously to the FDA-approved drugs (Figure S10). Compound **1**, an analogue of PRO, was 3-fold more potent than PRO as an Eis inhibitor (Table 1), an improvement by rational design. On the other hand, the IC_{50} values of compounds **2** and **3** were 5- and >7-fold higher than that of PRO, respectively (Table 1).

Crystal structures of Eis in complexes with compounds 1, 2, and 3.

We examined how compounds **1**, **2**, and **3** were bound to Eis, by determining the crystal structures of Eis in complexes with these compounds (Table S3, Figure 4). The bound **1** was well resolved in the omit F_o-F_c electron density map (Figure S11G). The chlorophenyl moiety was bound in the hydrophobic pocket similarly to that of PRO, as predicted (Figure 4A). The hydrazone-guanidinyl portion was bound in the conformation resembling to the second conformation of the biguanide of PRO, where the guanidinyl of **1** was stacked with the indole ring of Trp36, engaging in a π-cation interaction, while making a salt bridge with the terminal carboxyl of Eis. Likely because **1** lacked an isopropyl group present in PRO, which did not seem to fit properly into the binding pocket, **1** was observed in a single conformation and was 3-fold more potent than PRO in inhibiting Eis. This example showcases basic structure-based design principles.

Compounds **2** and **3** were bound to Eis with the well resolved fluorophenyl moieties bound in the hydrophobic pocket (Figure S11H,I) so that the fluorine was in the same location for both compounds (Figure 4B,C), also approximately coincident with the chlorine atom of the bound compound **1**. As a result, the hydrazone linker path had a minor difference, as the chlorophenyl moiety in compounds was also located in the same site for both bound molecules. For **2**, the conformation of the linker placed it too far to form a hydrogen bond with the hydroxyl group of Ser83 (Figure 4B), whereas for **3** the relevant N-O distance was appropriate (2.9 Å; Figure 4C). The chlorophenyl moiety was well resolved for compound **3** (Figure S11I), where it interacted with the indole ring of Trp36 and the side chain of Ile28 (Figure 4B). The linker in both **2** and **3** was apparently too long to allow ideal parallel stacking between the chlorophenyl rings of these compounds and the indole of Trp36, placing a part of the ring in a charged environment of the carboxyl groups of Glu401 and the C-terminus. The chlorophenyl ring of **2** was largely disordered (Figure S11H), likely

because rotational dynamics due to the above unfavorable interactions and the lack of the hydrogen bond that would stabilize the hydrazone linker. These structures suggest that the unfavorable interactions of the chlorophenyl moiety of **2** and **3** with Eis account for their weak enzyme inhibition.

Kinetic analysis of inhibition.

We investigated the mode of inhibition and determined the for all but the weak inhibitors VEN and compound **3** by carrying out the Michaelis-Menten analysis of KAN acetylation by Eis at different inhibitor concentrations (Figures 5 and 6 and Table S1). An unbiased analysis for each inhibitor was performed by a global nonlinear regression of all the data using the mixed mode of inhibition. This analysis yielded the best-fit values for the equilibrium constants of inhibitor binding to free enzyme (K_i) and to the enzyme-substrate complex ($K_{i,u}$; Table 1). Where only the former or the latter value could be determined with statistical significance, the mode was established as competitive or uncompetitive, respectively. AZL, CHQ, PRO, and compound **1** were competitive inhibitors with respect to KAN. Binding of AZL and CHQ to enzyme-substrate complex had a weak statistical significance as judged by the p-values and confidence intervals (Table 1), and it was of a much lower affinity than to free enzyme. MEF was a noncompetitive inhibitor, with $K_{i,} \approx K_{i,u}$, while compound **2** was uncompetitive. As described in the previous section, MEF did not appear to clash significantly with the aminoglycoside substrate (which would presumably allow MEF to bind Eis in the presence of bound KAN), while considerably remodeling the substrate binding site. This remodeling likely interfered with the catalysis. We described that the chlorophenyl moiety of **2**, which would cause minor steric hindrance for aminoglycoside binding, was not stably associated with Eis and was partially solvent exposed. Due to the conformational flexibility and a relatively small size of **2**, bound KAN and **2** could both be accommodated in the binding site, stabilizing each other, as indicated by the kinetic data. As with our previous attempts to crystallize the Eis-KAN complex, our efforts to crystallize Eis in complex with KAN in the presence of **2** did not yield electron density for KAN. We explain this by multiple binding modes of KAN to Eis, as evidenced by its acetylation by Eis at different positions in a random order.[7] Although a weak inhibitor, compound **2** is the first example of an uncompetitive Eis inhibitor, with the structure illustrating that a hydrophobic pocket in the vicinity of a substrate binding site can, in principle, be used to design uncompetitive inhibitors. Such rational design would be complicated since the inhibitors would directly interact with and stabilize the substrate (or the product); hence, predicting the inhibitor pose and interaction can be challenging.

Evaluation of compounds in *M. tuberculosis* cultures.

The Eis inhibitors were tested for their inhibition of growth of *Mtb* mc^{2}6230,[34] a BSL-2 *Mtb* strain derived from strain H37Rv. Some of the previously reported Eis inhibitors were observed to be toxic to H37Rv even in the absence of an aminoglycoside,[20] by an unknown mechanism. In this study, we identified MEF and CHQ to have MIC values of 16 μM and 64 μM, respectively (Table 1). The MEF MIC value was consistent with a previous report of modest inhibitory activity of MEF against a large panel of *Mtb* clinical isolates.[35] Inhibition of Eis cannot explain this effect, because Eis is not essential for *Mtb* growth *in vitro*.[36] None of the other compounds inhibited the growth of *Mtb* mc^{2}6230 at the highest concentration

tested (64 μM) (Table 1). We also tested if the Eis inhibitors behaved as KAN adjuvants by using our previously engineered *Mtb* strain mc^{2}6230 K204.[22] This strain harbored a point mutation in the *eis* promoter upregulating the expression of *eis* and rendering this strain KAN-resistant (Table 1), analogously to its H37Rv counterpart.[11] For this experiment, we measured the MIC of KAN in the absence and in the presence of Eis inhibitors at concentrations equal to their respective ½× MIC values or at 64 μM for all other compounds at four KAN concentrations in a clinically relevant range (10, 5, 2.5, and 1.25 μg/mL). Even though some synergy with KAN cannot be ruled out, in this range KAN remained inactive against the mycobacteria, indicating that these compounds did not inhibit Eis to a significant extent. The lack of Eis inhibition in the mycobacterial cells could be due to poor penetration of these compounds through the thick and waxy mycobacterial envelope. The toxicity of MEF and CHQ limited their concentrations to those near their IC_{50} values for Eis. For this reason, even if these molecules could reach cytoplasmic Eis, the partial Eis inhibition might not have been sufficient to observe significant synergy with KAN.

Evaluation of inhibitor selectivity.

Selectivity of the inhibitors was characterized by testing whether they inhibited NEO acetylation by other aminoglycoside acetyltransferases (AACs) that shared the basic GNAT fold with the catalytic domain of Eis, but differed in the structures of the substrate binding sites, the presence of other domains, and in their quaternary structures. We tested AZL, CHQ, MEF, and PRO with AAC(6')-Ie, AAC(2')-Ic, and AAC(3)-IV. All three acetylating enzymes were not inhibited by any of the Eis inhibitors at concentrations up to 200 μM. This result indicated that the compounds were selective inhibitors of Eis.

CONCLUSIONS

Repositioning of approved drugs is a potentially cost-effective strategy to aid in the development of new treatment regime for TB, especially useful considering that many TB patients worldwide cannot afford expensive medication. Our combined HTS-driven approach in searching for inhibitors identified five compounds that can block the acetylation activity of Eis, a drug resistance factor and compete with an aminoglycoside substrate. Among these inhibitors are AZL, VEN, PRO, CHQ, and MEF. Repositioning of antimalarial drugs CHQ and MEF as anti-TB drugs was recently discussed.[37] Our crystallographic studies indicated that these compounds bind in the substrate binding cavity explaining their modes of inhibition established by the kinetic analysis. Further medicinal chemistry optimization of these Eis inhibitors as aminoglycoside adjuvants is clearly needed to improve the penetration of the *Mtb* envelope by the analogues of these compounds.

Supplementary Material

Refer to Web version on PubMed Central for supplementary material.

ACKNOWLEDGMENTS

This study was funded by grants from the National Institutes of Health (NIH) AI090048 (to S.G.-T.), the Firland Foundation (to S.G.-T.), and the Center for Chemical Genomics (CCG) at the University of Michigan (to S.G.-T.), as well as by startup funds from the College of Pharmacy at the University of Kentucky (to S.G.-T. and O.V.T).

We acknowledge S. Vander Roest, M. Larsen, and P. Kirchhoff from the CCG at the University of Michigan for their help with HTS. We also would like to extend our appreciation to Abdelrahman S. Mayhoub for helping with the selection of FDA-approved drugs for screening. We thank the staff of sector SER-CAT of the Advanced Photon Source at the Argonne National Laboratories for assistance with remote X-ray diffraction data collection. The synchrotron access was supported, in part, by the Center for Structural Biology at the University of Kentucky. We thank the College of Pharmacy NMR Center (University of Kentucky) for NMR support. The findings and conclusions in this report are those of the authors and do not necessarily represent the views of the funding agencies.

REFERENCES

1. World Health Organization Fact Sheet 2022 (Tuberculosis). https://www.who.int/news-room/fact-sheets/detail/tuberculosis.
2. Deutsch-Feldman M; Pratt RH; Price SF; Tsang CA; Self JL Tuberculosis - United States, 2020. MMWR Morb. Mortal. Wkly Rep 2021, 70, 409–414. [PubMed: 33764959]
3. Kwak N; Hwang SS; Yim JJ Effect of COVID-19 on tuberculosis notification, South Korea. Emerg. Infect. Dis 2020, 26, 2506–2508. [PubMed: 32672531]
4. Uplekar M; Raviglione M WHO's end TB strategy: From stopping to ending the global TB epidemic. Indian J. Tuberc 2015, 62, 196–199. [PubMed: 26970458]
5. Chen W; Biswas T; Porter VR; Tsodikov OV; Garneau-Tsodikova S Unusual regioversatility of acetyltransferase Eis, a cause of drug resistance in XDR-TB. Proc. Natl. Acad. Sci., U. S. A 2011, 108, 9804–9808. [PubMed: 21628583]
6. Chen W; Green KD; Tsodikov OV; Garneau-Tsodikova S Aminoglycoside multiacetylating activity of the enhanced intracellular survival protein from *Mycobacterium smegmatis* and its inhibition. Biochemistry 2012, 51, 4959–4967. [PubMed: 22646013]
7. Houghton JL; Biswas T; Chen W; Tsodikov OV; Garneau-Tsodikova S Chemical and structural insights into the regioversatility of the aminoglycoside acetyltransferase Eis. ChemBioChem 2013, 14, 2127–2135. [PubMed: 24106131]
8. Green KD; Biswas T; Chang C; Wu R; Chen W; Janes BK; Chalupska D; Gornicki P; Hanna PC; Tsodikov OV; Joachimiak A; Garneau-Tsodikova S Biochemical and structural analysis of an Eis family aminoglycoside acetyltransferase from *Bacillus anthracis*. Biochemistry 2015, 54, 3197–3206. [PubMed: 25928210]
9. Green KD; Pricer RE; Stewart MN; Garneau-Tsodikova S Comparative study of Eis-like enzymes from pathogenic and nonpathogenic bacteria. ACS Infect. Dis 2015, 1, 272–283. [PubMed: 27622743]
10. Houghton JL; Green KD; Pricer RE; Mayhoub AS; Garneau-Tsodikova S Unexpected *N*-acetylation of capreomycin by mycobacterial Eis enzymes. J. Antimicrob. Chemother 2013, 68, 800–805. [PubMed: 23233486]
11. Zaunbrecher MA; Sikes RD Jr.; Metchock B; Shinnick TM; Posey JE Overexpression of the chromosomally encoded aminoglycoside acetyltransferase eis confers kanamycin resistance in *Mycobacterium tuberculosis*. Proc. Natl. Acad. Sci., U. S. A 2009, 106, 20004–20009. [PubMed: 19906990]
12. Campbell PJ; Morlock GP; Sikes RD; Dalton TL; Metchock B; Starks AM; Hooks DP; Cowan LS; Plikaytis BB; Posey JE Molecular detection of mutations associated with first- and second-line drug resistance compared with conventional drug susceptibility testing of *Mycobacterium tuberculosis*. Antimicrob. Agents Chemother 2011, 55, 2032–2041. [PubMed: 21300839]
13. Reeves AZ; Campbell PJ; Sultana R; Malik S; Murray M; Plikaytis BB; Shinnick TM; Posey JE Aminoglycoside cross-resistance in *Mycobacterium tuberculosis* due to mutations in the 5' untranslated region of whiB7. Antimicrob. Agents Chemother 2013, 57, 1857–1865. [PubMed: 23380727]
14. Green KD; Chen W; Garneau-Tsodikova S Identification and characterization of inhibitors of the aminoglycoside resistance acetyltransferase Eis from *Mycobacterium tuberculosis*. ChemMedChem 2012, 7, 73–77. [PubMed: 21898832]
15. Willby MJ; Green KD; Gajadeera CS; Hou C; Tsodikov OV; Posey JE; Garneau-Tsodikova S Potent inhibitors of zcetyltransferase Eis *overcome kanamycin resistance in Mycobacterium tuberculosis*. ACS Chem. Biol 2016, 11, 1639–1646. [PubMed: 27010218]

16. Garzan A; Willby MJ; Green KD; Gajadeera CS; Hou C; Tsodikov OV; Posey JE; Garneau-Tsodikova S Sulfonamide-based inhibitors of aminoglycoside acetyltransferase Eis abolish resistance to kanamycin in *Mycobacterium tuberculosis*. J. Med. Chem 2016, 59, 10619–10628. [PubMed: 27933949]

17. Garzan A; Willby MJ; Green KD; Tsodikov OV; Posey JE; Garneau-Tsodikova S Discovery and optimization of two Eis inhibitor families as kanamycin adjuvants against drug-resistant *M. tuberculosis*. ACS Med. Chem. Lett 2016, 7, 1219–1221. [PubMed: 27994767]

18. Garzan A; Willby MJ; Ngo HX; Gajadeera CS; Green KD; Holbrook SY; Hou C; Posey JE; Tsodikov OV; Garneau-Tsodikova S Combating enhanced intracellular survival (Eis)-mediated kanamycin resistance of *Mycobacterium tuberculosis* by novel pyrrolo[1,5-a]pyrazine-based Eis inhibitors. ACS Infect. Dis 2017, 3, 302–309. [PubMed: 28192916]

19. Ngo HX; Green KD; Gajadeera CS; Willby MJ; Holbrook SYL; Hou C; Garzan A; Mayhoub AS; Posey JE; Tsodikov OV; Garneau-Tsodikova S Potent 1,2,4-triazino[5,6 b]indole-3-thioether inhibitors of the kanamycin resistance enzyme Eis from *Mycobacterium tuberculosis*. ACS Infect. Dis 2018, 4, 1030–1040. [PubMed: 29601176]

20. Punetha A; Ngo HX; Holbrook SYL; Green KD; Willby MJ; Bonnett SA; Krieger K; Dennis EK; Posey JE; Parish T; Tsodikov OV; Garneau-Tsodikova S Structure-guided optimization of inhibitors of acetyltransferase Eis from *Mycobacterium tuberculosis*. ACS Chem. Biol 2020, 15, 1581–1594. [PubMed: 32421305]

21. Pang AH; Green KD; Chandrika NT; Garzan A; Punetha A; Holbrook SYL; Willby MJ; Posey JE; Tsodikov OV; Garneau-Tsodikova S Discovery of substituted benzyloxy-benzylamine inhibitors of acetyltransferase Eis and their anti-mycobacterial activity. Eur. J. Med. Chem 2022, 242, 114698. [PubMed: 36037791]

22. Punetha A; Green KD; Garzan A; Thamban Chandrika N; Willby MJ; Pang AH; Hou C; Holbrook SYL; Krieger K; Posey JE; Parish T; Tsodikov OV; Garneau-Tsodikova S Structure-based design of haloperidol analogues as inhibitors of acetyltransferase Eis from *Mycobacterium tuberculosis* to overcome kanamycin resistance. RSC Med. Chem 2021, 12, 1894–1909. [PubMed: 34825186]

23. Ashburn TT; Thor KB Drug repositioning: Identifying and developing new uses for existing drugs. Nat. Rev. Drug Discov 2004, 3, 673–683. [PubMed: 15286734]

24. Pantziarka P; Bouche G; Meheus L; Sukhatme V; Sukhatme VP; Vikas P The Repurposing Drugs in Oncology (ReDO) project. Ecancermedicalscience 2014, 8, 442. [PubMed: 25075216]

25. Green KD; Punetha A; Hou C; Garneau-Tsodikova S; Tsodikov OV Probing the robustness of inhibitors of tuberculosis aminoglycoside resistance enzyme Eis by mutagenesis. ACS Infect. Dis 2019, 5, 1772–1778. [PubMed: 31433614]

26. Otwinowski Z; Minor W Processing of X-ray diffraction data collected in oscillation mode. Methods Enzymol. 1997, 276, 307–326. [PubMed: 27754618]

27. McCoy AJ; Grosse-Kunstleve RW; Adams PD; Winn MD; Storoni LC; Read RJ Phaser crystallographic software. J. Appl. Crystallogr 2007, 40, 658–674. [PubMed: 19461840]

28. Emsley P; Cowtan K Coot: Model-building tools for molecular graphics. Acta Crystallogr. D 2004, 60, 2126–2132. [PubMed: 15572765]

29. Murshudov GN; Vagin AA; Dodson EJ Refinement of macromolecular structures by the maximum-likelihood method. Acta Crystallogr. D 1997, 53, 240–255. [PubMed: 15299926]

30. Williams CJ; Headd JJ; Moriarty NW; Prisant MG; Videau LL; Deis LN; Verma V; Keedy DA; Hintze BJ; Chen VB; Jain S; Lewis SM; Arendall WB 3rd; Snoeyink J; Adams PD; Lovell SC; Richardson JS; Richardson DC MolProbity: More and better reference data for improved all-atom structure validation. Protein Sci. 2018, 27, 293–315. [PubMed: 29067766]

31. Green KD; Chen W; Houghton JL; Fridman M; Garneau-Tsodikova S Exploring the substrate promiscuity of drug-modifying enzymes for the chemoenzymatic generation of *N*-acylated aminoglycosides. ChemBioChem 2010, 11, 119–126. [PubMed: 19899089]

32. British national formulary: BNF 76 (76 ed.). Pharmaceutical Press. 2018. *p*. 1169. ISBN 9780857113382..

33. Xue Y; Zhang S; Yang Y; Lu M; Wang Y; Zhang T; Tang M; Takeshita H Acute pulmonary toxic effects of chlorhexidine (CHX) following an intratracheal instillation in rats. Hum. Exp. Toxicol 2011, 30, 1795–1803. [PubMed: 21339254]

34. Sambandamurthy VK; Derrick SC; Hsu T; Chen B; Larsen MH; Jalapathy KV; Chen M; Kim J; Porcelli SA; Chan J; Morris SL; Jacobs WR Jr. *Mycobacterium tuberculosis* DeltaRD1 DeltapanCD: A safe and limited replicating mutant strain that protects immunocompetent and immunocompromised mice against experimental tuberculosis. Vaccine 2006, 24, 6309–20. [PubMed: 16860907]

35. Krieger D; Vesenbeckh S; Schonfeld N; Bettermann G; Bauer TT; Russmann H; Mauch H Mefloquine as a potential drug against multidrug-resistant tuberculosis. Eur. Respir. J 2015, 46, 1503–1505. [PubMed: 26206875]

36. Samuel LP; Song CH; Wei J; Roberts EA; Dahl JL; Barry CE; Jo EK; Friedman RL Expression, production and release of the Eis protein by *Mycobacterium tuberculosis* during infection of macrophages and its effect on cytokine secretion. Microbiology (Reading) 2007, 153, 529–540. [PubMed: 17259625]

37. An Q; Li C; Chen Y; Deng Y; Yang T; Luo Y Repurposed drug candidates for antituberculosis therapy. Eur. J. Med. Chem 2020, 192, 112175. [PubMed: 32126450]

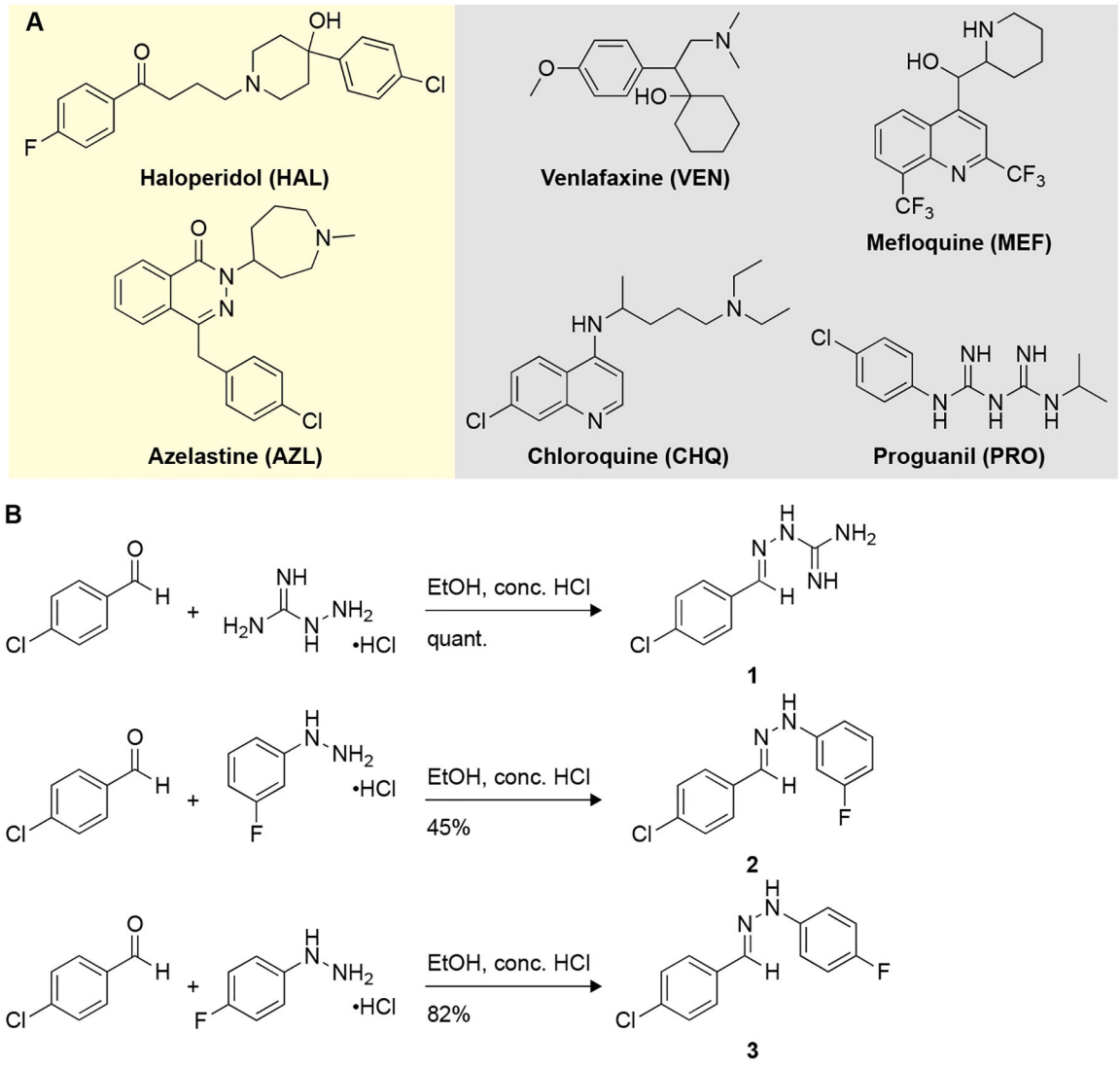

Figure 1.

Chemical structures of Eis inhibitors. **A**. Two hits (HAL[22] and AZL) found by screening the ~2,500 HTS compound library (yellow box), and the other four FDA-approved drugs (VEN, MEF, CHQ, and PRO) originated from a rationally selected 20 compound library (grey box). **B**. The synthetic scheme used for the preparation of PRO analogues **1**-**3**.

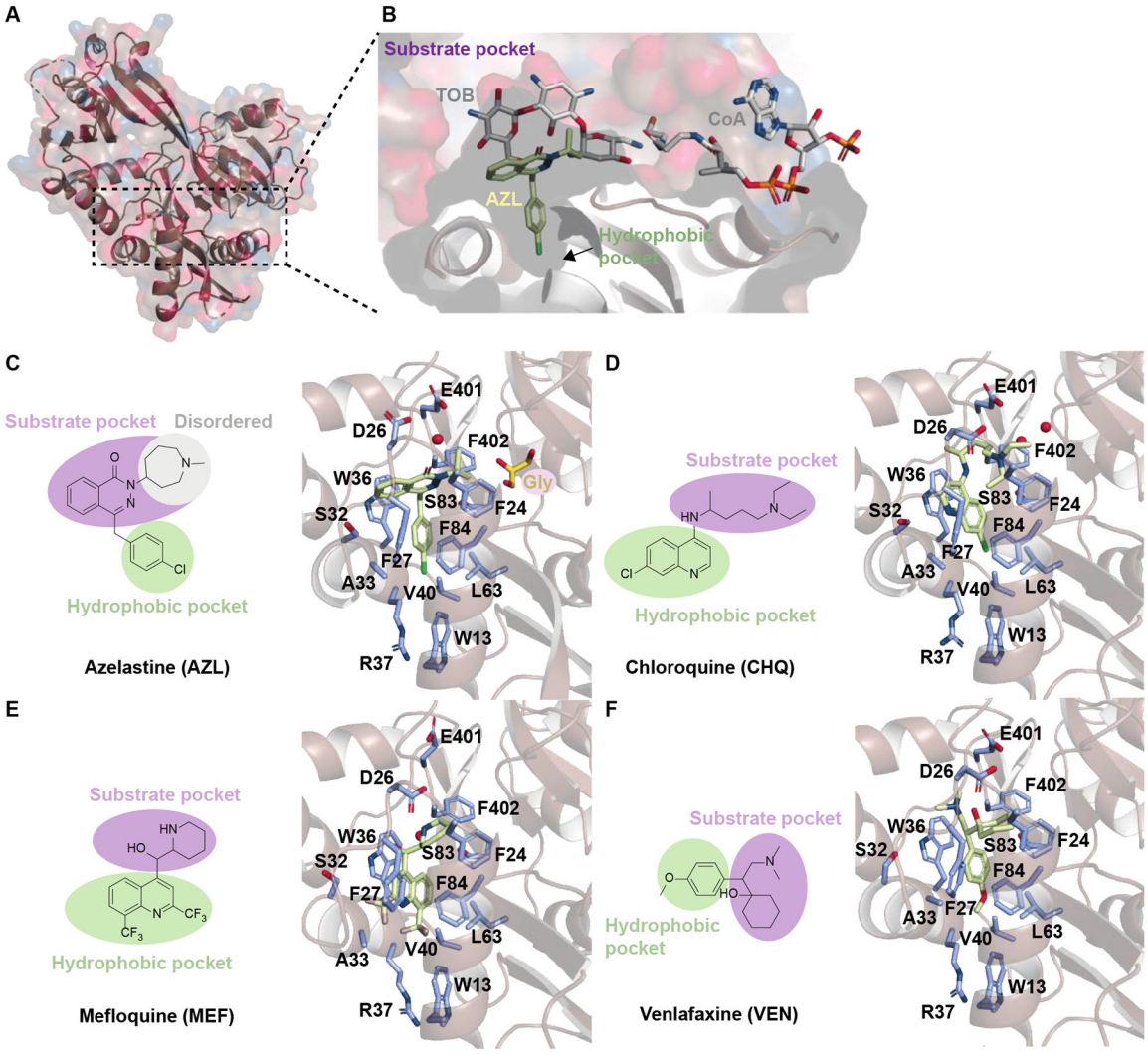

Figure 2.

Crystal structures of Eis in complexes with AZL, CHQ, MEF, and VEN. **A**. The overall view of an Eis C204A protomer in complex with AZL. **B**. A magnified view of the dotted box in panel **A**, showing the bound AZL and superimposed tobramycin (TOB) and CoA from our previously reported structure of the Eis-TOB complex (PDB ID: 4JD6). Panels **C**, **D**, **E**, and **F** show the chemical structures of the inhibitors with the schematic of the binding pocket (left) and the magnified views of the Eis-inhibitor interfaces in the respective crystal structures (right) for AZL, CHQ, MEF, and VEN, respectively. The inhibitors are shown as yellow sticks, the residues interacting with the inhibitors as blue sticks, and water molecules as red balls.

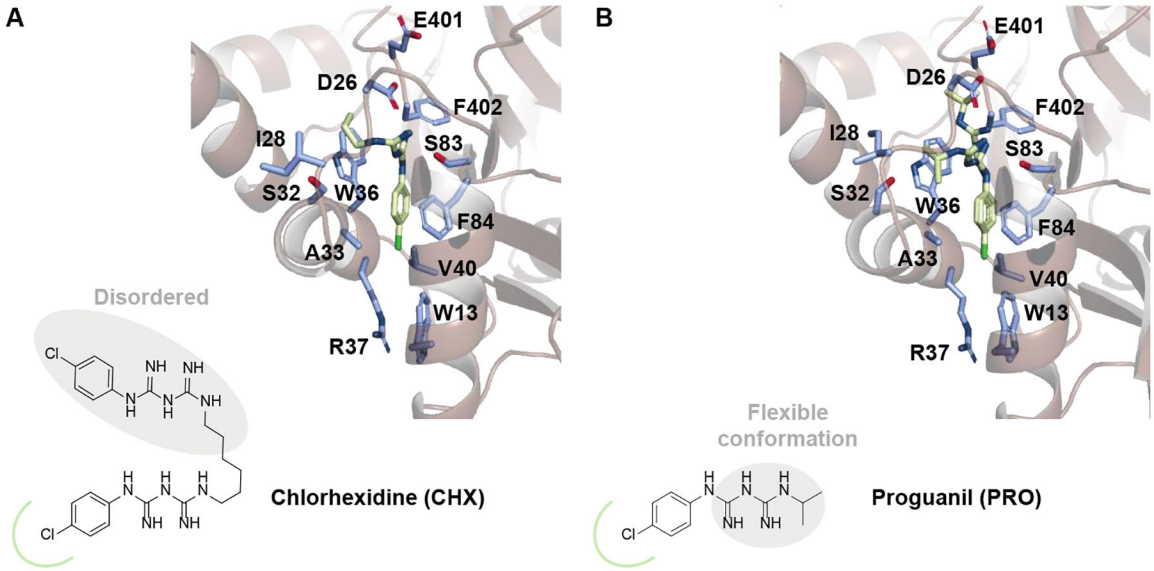

Figure 3.

Magnified views of the Eis-inhibitor interfaces for CHX and PRO. **A**. The Eis-CHX interface. **B**. The Eis-PRO interface. The chemical structures of the inhibitors are shown in the lower left corners of the respective panels, with the part of the structure bound in the hydrophobic pocket indicated by a green curve. The inhibitors are shown as yellow sticks, and the Eis residues surrounding the inhibitors as blue sticks.

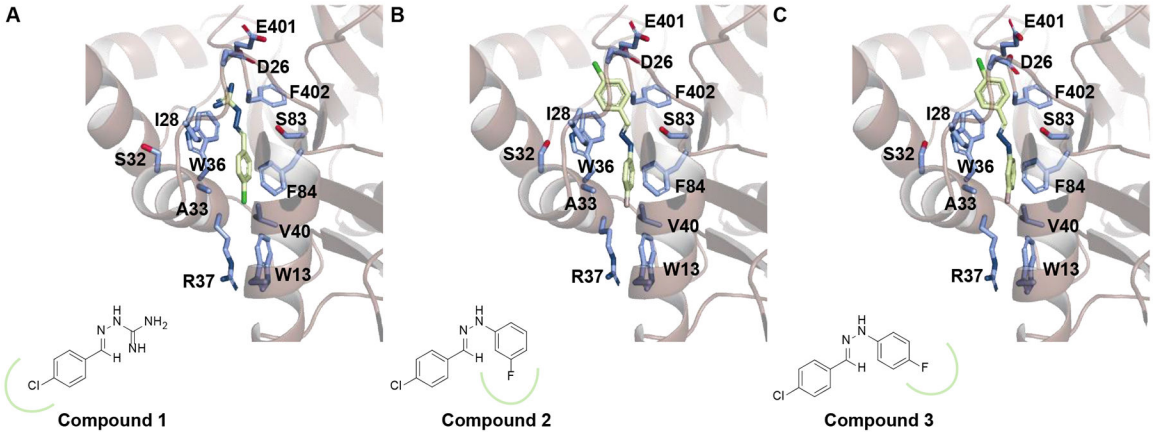

Figure 4.

Magnified views of the Eis-inhibitor interfaces for compounds **1**, **2**, and **3**. **A**. The Eis-**1** interface. **B**. The Eis-**2** interface. **C**. The Eis-**3** interface. The chemical structures of the inhibitors are shown in the lower left corners of the respective panels, with the part of the structure bound in the hydrophobic pocket indicated by a green curve. The inhibitors are shown as yellow sticks, and the Eis residues surrounding the inhibitors as blue sticks.

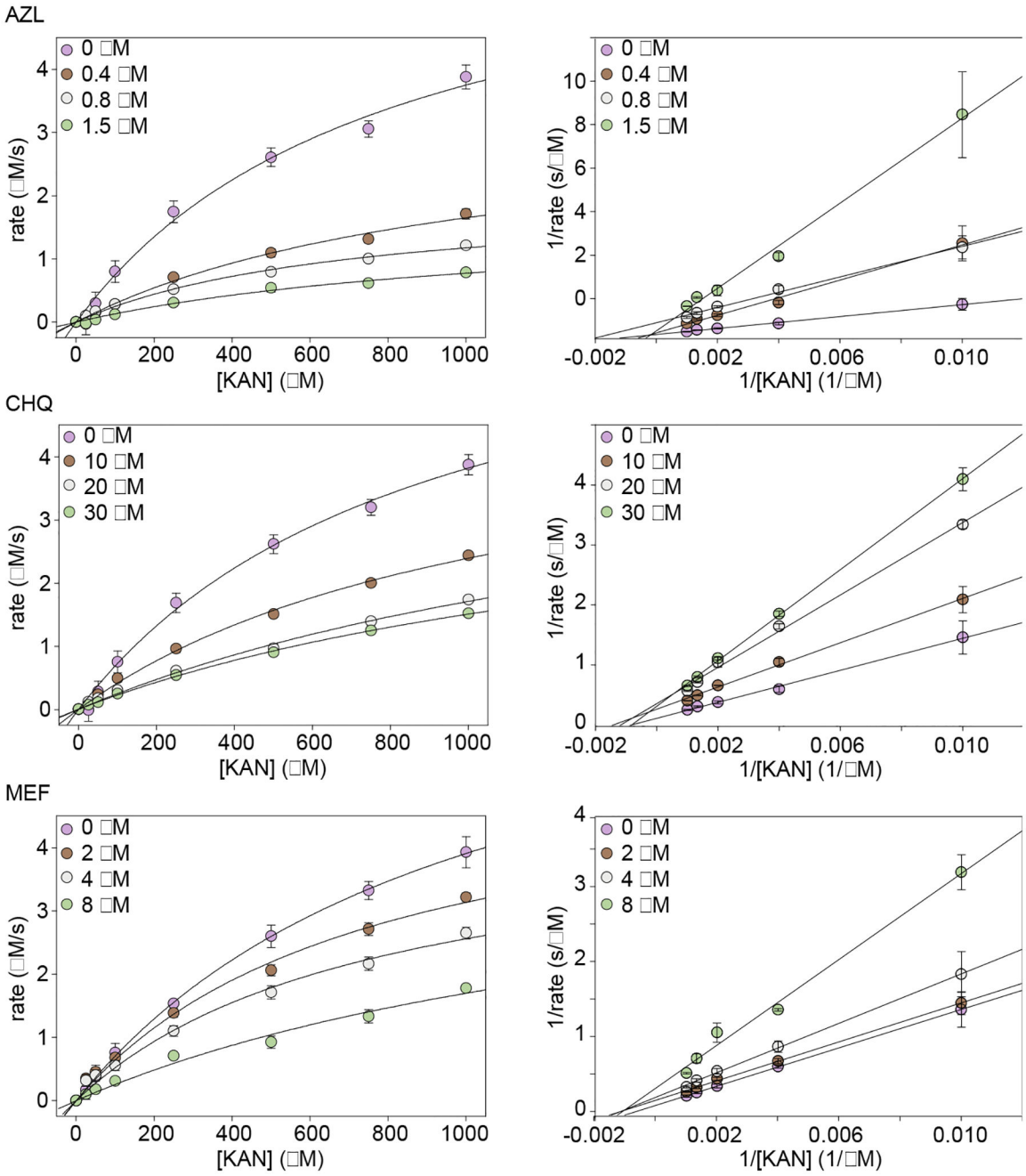

Figure 5.

Mode of inhibition of AZL, CHQ, and MEF. The Michaelis-Menten curves (left) and Lineweaver-Burk plots (right) illustrated the modes of inhibition of the compounds.

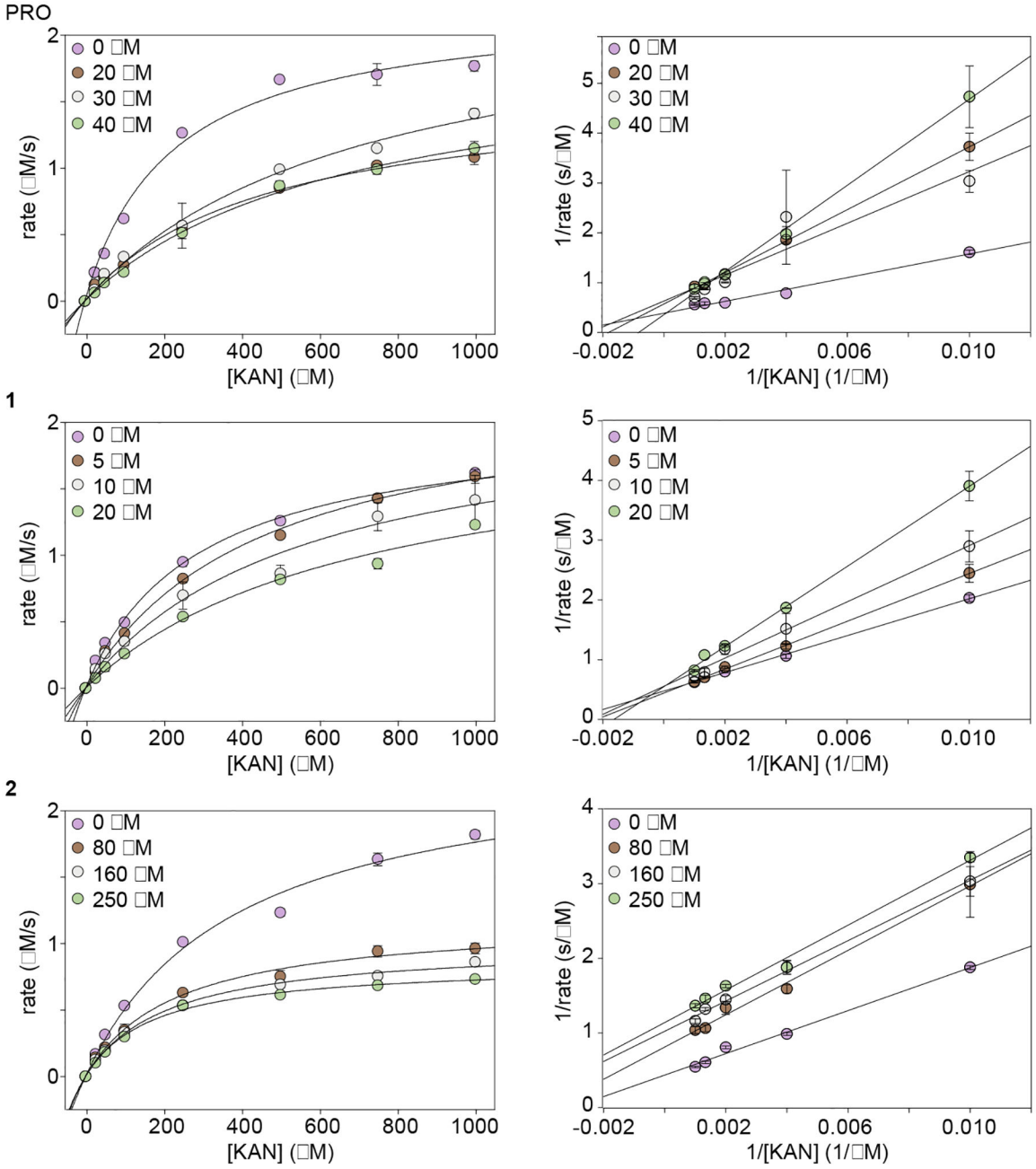

Figure 6.

Mode of inhibition of PRO, **1**, and **2**. The Michaelis-Menten curves (left) and Lineweaver-Burk plots (right) illustrated competitive inhibition of the PRO and compound **1**, but uncompetitive inhibition for compound **2**.

Table 1.

Activity of KAN and tested compounds in the Eis acetylation assays and in *Mtb* mc^{2}6230 culture growth assays.

Compounds	**IC_{50} (μM)**	**K_i (μM)[a]**	**$K_{i,u}$ (μM)[b]**	**MIC (μM) mc^{2}6230**	**MIC_{KAN} (μg/mL) mc^{2}6230**	**MIC_{KAN} (μg/mL) mc^{2}6230 K204**
Azelastine (AZL)	0.79 ± 0.08	0.24 ± 0.05	0.9 ± 0.5 (p = 0.08)	32	≤ 1.25	> 10
Venlafaxine (VEN)	134 ± 21	N/D	N/D	> 64	≤ 1.25	> 10
Chloroquine (CHQ)	20 ± 2	12.3 ± 2.7	35 ± 20 (p = 0.1)	64	≤ 1.25	> 10
Mefloquine (MEF)	4.2 ± 0.8	7.2 ± 1.1	5.9 ± 1.3 (p = 0.0002)	16	≤ 1.25	> 10
Proguanil (PRO)	30 ± 7	28 ± 10	N/D	> 64	≤ 1.25	> 10
1	10 ± 3	17.0 ± 2.4	N/D	> 64	≤ 1.25	> 10
2	160 ± 49	N/D	104 ± 8	> 64	≤ 1.25	> 10
3	> 200	N/D	N/D	> 64	≤ 1.25	> 10
Chlorhexidine (CHX)	0.67 ± 0.19[c]			≤ 0.03[a]	N/D	N/D
Kanamycin (KAN)				0.17	0.1	320
Isoniazid (INH)				≤ 3.6		

[a]The equilibrium constant for inhibitor binding to free enzyme.

[b]The equilibrium constant for inhibitor binding to enzyme-substrate complex.

[c]A previously published value.[14]

N/D = Not determined.